Cellular/Molecular

The Actin-Binding Protein Abp1 Controls Dendritic Spine Morphology and Is Important for Spine Head and Synapse Formation

Akvile Haeckel,[1] Rashmi Ahuja,[1] Eckart D. Gundelfinger,[2] Britta Qualmann,[1] and Michael M. Kessels[1]

[1]Institute for Biochemistry I, Friedrich Schiller University Jena, 07743 Jena, Germany, and [2]Department of Neurochemistry and Molecular Biology, Leibniz Institute for Neurobiology, 39118 Magdeburg, Germany

Polymerization and organization of actin into complex superstructures, including those found in dendritic spines, is indispensable for structure and function of neuronal networks. Here we show that the filamentous actin (F-actin)-binding protein 1 (Abp1), which controls Arp2/3 complex-mediated actin nucleation and binds to postsynaptic scaffold proteins of the ProSAP (proline-rich synapse-associated protein 1)/Shank family, has a profound impact on synaptic organization. Overexpression of the two Abp1 F-actin-binding domains increases the length of thin, filopodia-like and mushroom-type spines but dramatically reduces mushroom spine density, attributable to lack of the Abp1 Src homology 3 (SH3) domain. In contrast, overexpression of full-length Abp1 increases mushroom spine and synapse density. The SH3 domain alone has a dominant-negative effect on mushroom spines, whereas the density of filopodia and thin, immature spines remains unchanged. This suggests that both actin-binding and SH3 domain interactions are crucial for the role of Abp1 in spine maturation. Indeed, Abp1 knockdown significantly reduces mushroom spine and synapse density. Abp1 hereby works in close conjunction with ProSAP1/Shank2 and ProSAP2/Shank3, because Abp1 effects were suppressed by ProSAP2 RNA interference and the ProSAP/Shank-induced increase of spine head width is further promoted by Abp1 cooverexpression and reduced on Abp1 knockdown. Also, interfering with the formation of functional Abp1–ProSAP protein complexes prevents ProSAP-mediated spine head extension. Spine head extension furthermore depends on local Arp2/3 complex-mediated actin polymerization, which is controlled by Abp1 via the Arp2/3 complex activator N-WASP (neural Wiskott-Aldrich syndrome protein). Abp1 thus plays an important role in the formation and morphology control of synapses by making a required functional connection between postsynaptic density components and postsynaptic actin dynamics.

Key words: **postsynaptic density; actin cytoskeleton; synaptic scaffold; synapse formation; spine morphogenesis; ProSAP/Shank**

Introduction

Synapses are highly specialized and organized sites of cell–cell contact and communication, yet they are dynamic and exhibit a high degree of morphological plasticity. Such morphological changes ultimately require dynamics in the actin cytoskeleton, which represents the major structural component of the postsynaptic apparatus (Dillon and Goda, 2005; Schubert et al., 2006; Tada and Sheng, 2006). Excitatory synapses in the mammalian CNS frequently are localized on dendritic spines. For mature spines, a "mushroom-like" shape with thin necks and bulbous heads, on which synaptic contacts form, is characteristic. Major components of spine heads are elaborated actin cytoskeletal and cytomatrix structures, the postsynaptic density (PSD). The PSD contains high concentrations of cell adhesion molecules, neurotransmitter receptors, ion channels, and signal transduction proteins (Sheng and Sala, 2001; Kreienkamp, 2002; Boeckers, 2006). Intensive crosstalk of the actin cytoskeleton and cytomatrix proteins, which are connected to the machineries for cell adhesion and synaptic transmission within the PSD, is of high importance (Gundelfinger et al., 2003; Okamoto et al., 2004; Carlisle and Kennedy, 2005) because the complex postsynaptic protein network is not static but can respond to synaptic activity with massive reorganizations of both synaptic membrane components and the associated intracellular scaffold. The actin cytoskeleton plays an important role in these reorganizations, which are the basis for postsynaptic plasticity. Actin is a driving force behind the formation and morphological changes of postsynaptic spines (Matus, 2000; Schubert et al., 2006; Tada and Sheng, 2006).

With the actin-binding protein 1 (Abp1/SH3P7/HIP-55), we have identified a protein concentrated in postsynaptic compartments that binds to actin filaments (Kessels et al., 2000), is signal

Received Jan. 24, 2008; revised Aug. 16, 2008; accepted Aug. 26, 2008.

This work was supported by grants from the Katholischer Akademischer Austauschdienst (A.H.), Deutsche Forschungsgemeinschaft Grants QU116/2-3, QU116/2-4, and QU116/4-1, Kultusministerium Land Sachsen-Anhalt Grant XN3571A and the Schram Foundation (B.Q.), and Deutsche Forschungsgemeinschaft Grants KE685/2-2 and KE685/2-3 (M.M.K.). We thank K. Hartung and L. Schwintzer for technical support, C. Spilker and A. Fejtova for initial help with preparing primary neuronal cultures, R. Frischknecht for providing an mRFP-expressing plasmid (cloned into pc-DNA), C. Sala for providing the plasmid for ProSAP2 RNAi, T. Boeckers for providing plasmids encoding for ProSAP1–GFP and ProSAP2–GFP, and for anti-ProSAP1 and anti-ProSAP2 antibodies, M. Welch for providing anti-Arp3 antibodies, and W. D. Altrock and E. D. Gundelfinger for providing anti-Piccolo antibodies.

Correspondence should be addressed to Michael M. Kessels or Britta Qualmann, Institute for Biochemistry I, Friedrich Schiller University Jena, Nonnenplan 2, 07743 Jena, Germany. E-mail: michael.kessels@mti.uni-jena.de or britta.qualmann@mti.uni-jena.de.

DOI:10.1523/JNEUROSCI.0336-08.2008

 0270-6474/08/2810031-14$15.00/0

responsive (Larbolette et al., 1999; Kessels et al., 2000, 2001; Han et al., 2003; Le Bras et al., 2004) and interacts directly with ProSAP (proline-rich synapse-associated protein 1)/Shanks (Qualmann et al., 2004), major PSD scaffolding proteins (Sheng and Kim, 2000; Boeckers et al., 2002). Whereas the direct association of Abp1 with filamentous action (F-actin) occurs through two independently working N-terminal domains (Kessels et al., 2000), a C-terminal Src homology 3 (SH3) domain mediates the interaction with ProSAP1/Shank2 and ProSAP2/Shank3 (Qualmann et al., 2004). Importantly, Abp1 associates with dynamic cortical actin filaments and ProSAPs/Shanks simultaneously and is incorporated into ProSAP/Shank-positive synapses as a consequence of previous synaptic stimulation (Qualmann et al., 2004). These results prompted us to propose that Abp1–ProSAP/Shank complexes serve to connect synaptic signal reception to postsynaptic structural plasticity via rearrangements of the actin cytoskeleton in spines. This idea is also supported by the fact that Abp1 explicitly interacts with dynamic F-actin structures but not with more static ones (Kessels et al., 2000) and controls the activity of the Arp2/3 complex, which nucleates new actin filaments (Pinyol et al., 2007). In this study, we experimentally addressed the hypothesis of a role of Abp1 in spine organization and reveal that Abp1 plays a crucial role in the formation of mushroom-shaped spines and synapses. Abp1 hereby modulates spine morphology by both actin filament side binding and by providing a functional connection of a dynamic actin cytoskeleton with the ProSAP/Shank-based postsynaptic scaffold.

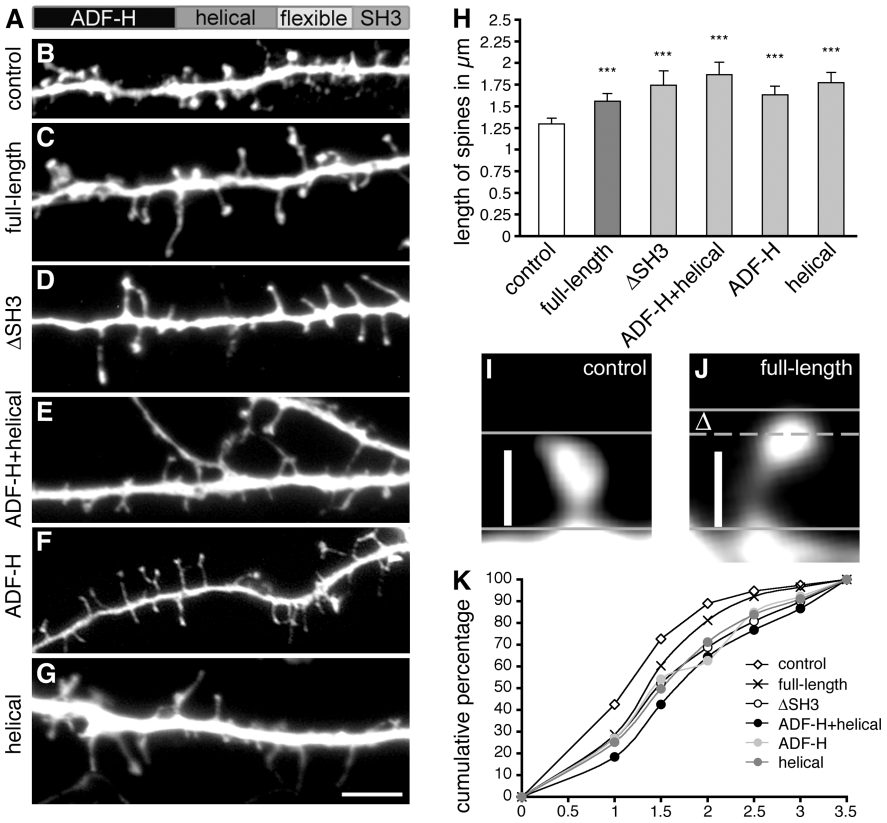

Figure 1. Expression of Abp1 full length and fragments thereof containing the F-actin binding domains induce increased spine length. ***A***, Domain structure of Abp1. ***B–G***, Images show the changes in spine morphology of hippocampal neurons at 14 DIV double-transfected at 12 DIV with GFP and full-length Abp1 or deletion constructs thereof. Compared with neurons transfected with GFP as control (***B***), neurons double transfected with myc-tagged Abp1 full-length (***C***), ΔSH3 (***D***), ADF-H+helical (***E***), ADF-H (***F***), and helical (***G***) show an increase in spine length. To make these effects obvious, the images shown also include extraordinarily long spines, which cannot be found in controls. In all cases, the GFP channel used to evaluate morphology is shown. Scale bar, 5 μm. ***H***, Mean of spine length (μm + SD) in neurons transfected with the constructs indicated obtained by quantitative analysis confirm that the spine elongation induced by Abp1 and its F-actin binding domains is highly significant. ***$p < 0.001$. ***I***, ***J***, Visualization of spines with sizes representing the average in the quantitative examinations (***H***) of control neurons (***I***) and of Abp1-overexpressing neurons (***J***), respectively. Vertical bar, 1 μm. Dashed line in ***J*** represents length of control for improved comparability. ***K***, Cumulative distribution of spine length (in micrometers) in neurons transfected with the constructs indicated.

Materials and Methods

DNA constructs. NH_2-terminally myc-tagged Abp1 constructs of full-length protein and deletion mutants (ΔSH3, ADF-H+helical, ADF-H, flex+SH3, flex-SH3^{mut}, and SH3) for overexpression in mammalian cells were described by Kessels et al. (2001). Additional deletion mutants, such as helical (amino acids 164–281) and SH3^{mut} [Abp1 SH3 domain harboring two point mutations (P422L and G425R) rendering it inactive for binding to proline-rich motifs (Kessels et al., 2001)] were generated by PCR from appropriate templates and cloned into the pRK5 vector similar to the mutants described previously (Kessels et al., 2001). Green fluorescent protein (GFP)–N-WASP C-terminal fragment (CA), RNA interference (RNAi) constructs directed against rat Abp1, the RNAi-resistant Abp1 mutant, the nonsilencing RNAi construct, and the constructs for Arp3 RNAi and N-WASP (neural Wiskott-Aldrich syndrome protein) RNAi were described by Pinyol et al. (2007). ProSAP1 pieces were generated by PCR and cloning into enhanced GFP vector (pEGFP). Deletion mutants were generated by fusion of pieces and cloning into pEGFP. Correct cloning was verified by sequencing.

ProSAP1 and ProSAP2 full-length constructs were kindly provided by T. Boeckers (University of Ulm, Ulm, Germany). The plasmid for ProSAP2 RNAi was described by Roussignol et al. (2005) and was kindly provided by C. Sala (Consiglio Nazionale delle Ricerche Institute of Neuroscience, University of Milan, Milan, Italy). Monomeric red fluorescent protein (mRFP) vector was kindly provided by R. Frischknecht (Leibniz Institute for Neurobiology, Magdeburg, Germany).

Antibodies and drugs. Polyclonal rabbit anti-Abp1 antibodies have been described previously (Fenster et al., 2003). Monoclonal anti-myc antibodies 9E10 were from Babco; polyclonal rabbit anti-myc antibodies were from Santa Cruz Biotechnology. Polyclonal rabbit anti-GFP antibodies, monoclonal anti-GFP antibodies, polyclonal rabbit NMDA2B antibodies, and monoclonal anti-PSD-95 antibodies were from Abcam. Monoclonal and polyclonal anti-synapsin antibodies were from Synaptic Systems. Polyclonal rabbit anti-Arp3 rabbit antibodies were kindly provided by M. D. Welch (University of California, Berkeley, Berkeley, CA), guinea pig anti-Piccolo antibodies were provided by W. D. Altrock and E. D. Gundelfinger (Leibniz Institute for Neurobiology, Magdeburg, Germany), and guinea pig anti-ProSAP1, guinea-pig anti-ProSAP2, and rabbit anti-ProSAP2 antibodies were provided by T. Boeckers. Polyclonal rabbit anti-RFP antibodies were from BD Biosciences and Millipore Bioscience Research Reagents.

Secondary antibodies used include the following: Alexa Fluor 350, 488, and 568 goat anti-mouse, Alexa Fluor 488, 350, and 568 goat anti-rabbit, Alexa Fluor 488 and 568 goat anti-guinea pig (Invitrogen), donkey anti-mouse Cy5 (cyanine 5) antibodies (Dianova), and peroxidase-conjugated anti-mouse antibodies (Dianova). Alexa Fluor 488 phalloidin was from Invitrogen.

Coprecipitation assays and coimmunoprecipitations. A fusion protein of

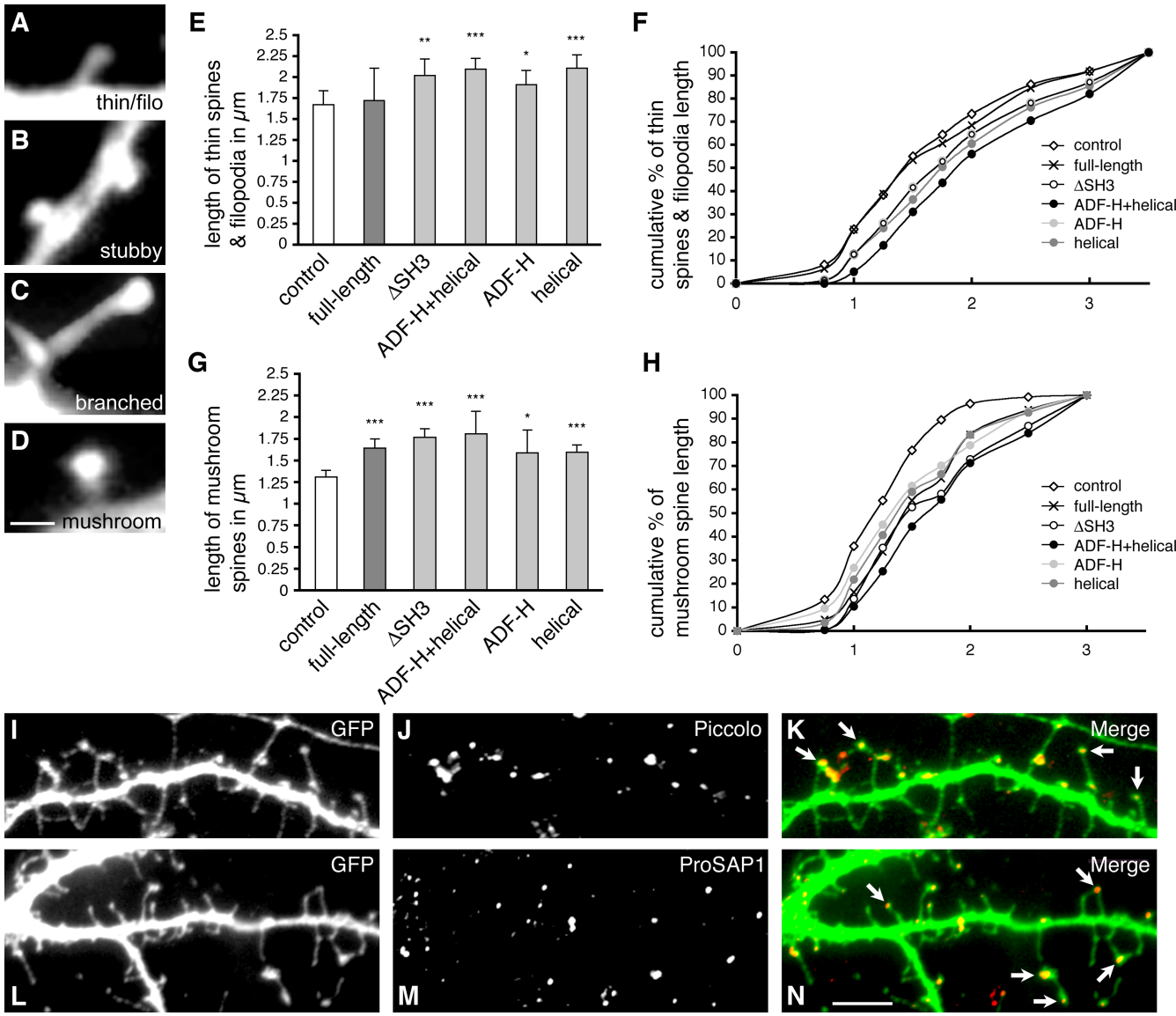

Figure 2. Abp1 overexpression results predominantly in elongation of mushroom-type spines. ***A–D***, Typical examples of thin (***A***), stubby (***B***), branched (***C***), and mushroom (***D***) types of spines. ***E–H***, Whereas the actin-binding domains of Abp1 increase the length of both thin spines and filopodia (***E***, ***F***) and mushroom spines (***G***, ***H***), overexpression of the full-length protein selectively affects the length of mushroom spines. The means of thin spines and filopodia length (***E***) and mushroom spine length (***G***) (μm + SD) as well as the cumulative distribution of thin spines and filopodia (***F***) and mushroom spine (***H***) length (in micrometers) in neurons transfected with the constructs indicated is depicted. *$p < 0.05$; **$p < 0.01$; ***$p < 0.001$. ***I–N***, Synaptic integration of spines morphologically altered by Abp1 overexpression. Primary hippocampal neurons were cotransfected with GFP as a volume marker (***I***, ***L***; green in merged images ***K*** and ***N***) and myc-tagged full-length Abp1 and stained at 14 DIV for presynaptic (Piccolo; ***J***; red in merged image ***K***) and postsynaptic (ProSAP1; ***M***; red in merged image ***N***) marker proteins. Arrows in the merged images ***K*** and ***N*** highlight elongated mushroom spines that contain the PSD component ProSAP1 (***N***) and are contacted by presynaptic active zones marked by Piccolo immunoreactivity (***K***), respectively. Scale bars: (in ***D***) ***A–D***, 1 μm; (in ***N***) ***I–N***, 5 μm.

the Abp1 SH3 domain with glutathione *S*-transferase (GST) and GST were purified from *Escherichia coli* as described previously (Qualmann and Kelly, 2000). Coprecipitation assays were done with immobilized GST–Abp1 SH3 domain and lysates of HEK293 cells expressing different ProSAP (deletion) mutants according to procedures described by Kessels and Qualmann (2002), Qualmann et al. (2004), and Kessels and Qualmann (2006), respectively. Every affinity purification experiment was accompanied by experiments with only GST instead of GST–Abp1 SH3 domain attached to the matrix to control for specificity.

Neuronal cell culture, transfection, and immunostaining. Hippocampal neuronal cultures were prepared as described previously by Pinyol et al. (2007). Neurons were transfected at 10–12 d *in vitro* (DIV) with Lipofectamine 2000 using 1–2 μg of DNA and 1 μg of reagent for one well of a 24-well plate and fixed after 48–80 h (14 DIV).

For all immunostaining experiments, the neurons were fixed in 4% formaldehyde in PBS, pH 7.45, for 6 min at room temperature. Immunostainings were performed according to Kessels et al. (2000) and Qualmann et al. (2004).

For quantification of Abp1 knockdown levels during transfection with RNAi constructs, the mean of fluorescence intensity of endogenous Abp1 was measured in nontransfected cells or pRNAT-transfected control cells and compared with that of cells transfected with Abp1 RNAi constructs, which were detectable by the fluorescence signal generated by the cell-filling molecule (GFP, mRFP) coexpressed from the bicistronic pRNAT vector.

Microscopy and quantitative analyses of spine morphology. Immunofluorescence images were acquired with a Carl Zeiss Axioplan 2 microscope equipped with a CCD camera 2.1.1 from Diagnostic Instruments and processed in MetaVue Software. Morphometric measurements were performed with the aid of NIH Image software (ImageJ). Each experiment

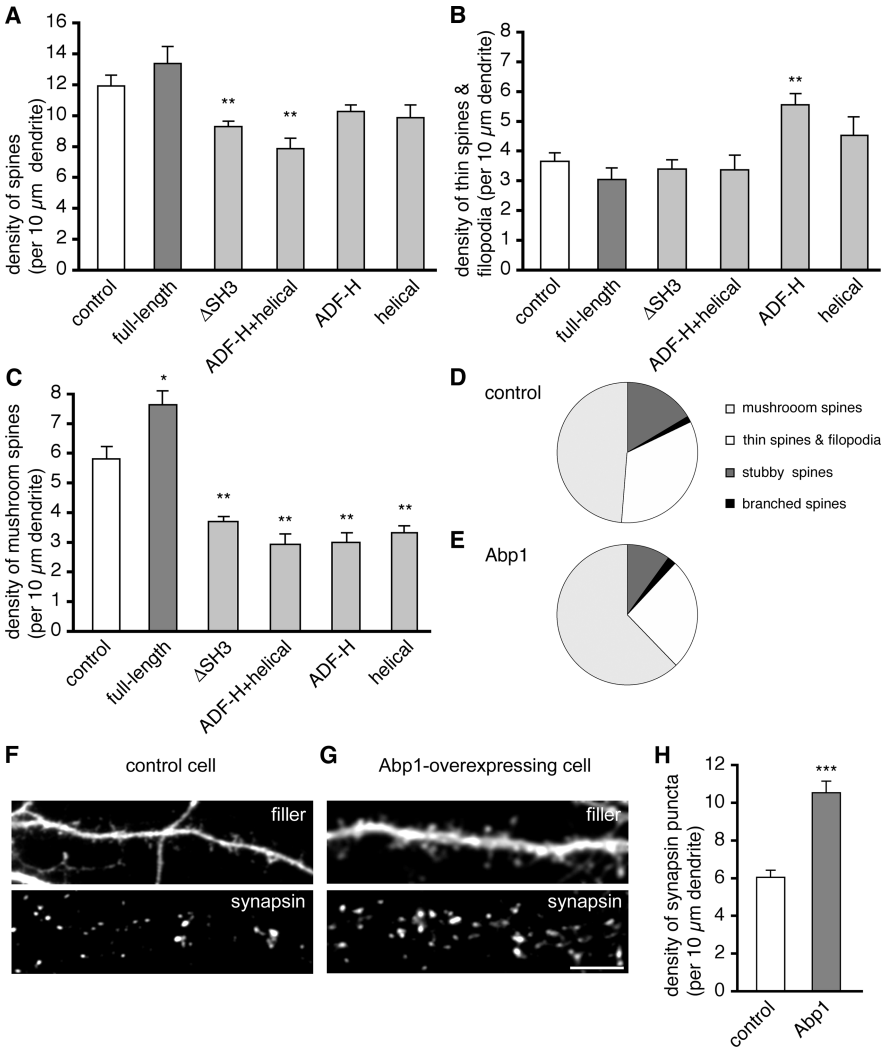

Figure 3. Effects of full-length Abp1 and actin interaction domains of Abp1 on the density of mushroom-shaped spines and synapses. ***A–C***, Diagrams depict the means + SEM for the density of spines of all types (***A***) and their individual morphology groups (***B***, thin spines and filopodia; ***C***, mushroom spines) for neurons transfected with a cell-filling molecule (GFP, mRFP) alone (control) as well as cotransfected with Abp1 and fragments thereof as indicated. $*p < 0.05$; $**p < 0.01$. ***D***, ***E***, Relative abundance of the four different spine classes in control (***D***) and Abp1-overexpressing neurons (***E***). ***F***, ***G***, Anti-synapsin immunostaining (bottom row) of synapses contacting control (***F***) and Abp1-overexpressing neurons (***G***). ***H***, Quantitation of synapse density, as defined by anti-synapsin immunostaining, in control and Abp1-overexpressing neurons show a highly significant increase in synapse density during Abp1 overexpression ($***p < 0.001$). Scale bar, 5 μm.

was performed on two to four independent coverslips and usually three times with independent neuronal preparations. To ensure maximal reliance and reproducibility, all experiments included the full set of the different controls (both positive and negative) for reference. Neurons for morphometric analyses were sampled quantitatively from each coverslip. In most cases, cells were cotransfected with GFP or mRFP to visualize detailed morphology and to outline the spines. Additional quantitative morphometric analyses as well as high-resolution double-labeling experiments confirmed that also myc–Abp1 immunoreactivity outlines the morphology of the cells in a manner indistinguishable from GFP and mRFP, respectively.

To determine spine size, 300–1000 spines (from 6–19 neurons) were measured for each condition. For spine length, the distance from the base of the neck to the furthest point on the spine head was measured. Spine group definitions are according to Hering and Sheng (2003). Heads of mushroom spines were measured taking the maximal width of the spine head perpendicular to the axis along the spine neck. For each condition, individual spine dimensions were grouped first and averaged per neuron; means from multiple individual neurons were then averaged to obtain a mean (SD and SEM, respectively) for the population of neurons.

For spine and synaptic puncta density measurements, all clearly evaluable areas of 50–100 μm of primary dendrites from each imaged neuron were used. This excludes a potential bias during area selection. Each individual spine present on the entire dendrite parts was included in the spine density examinations. For the determination of synapse number, each synapse highlighted by presynaptic markers and postsynaptic markers, respectively, was counted, i.e., synapses at both spines and dendrites were included.

Results

Abp1 increases longitudinal spine growth

ProSAP/Shank proteins are prominent scaffold proteins in the PSD that directly and indirectly interact with different membrane receptors and are furthermore connected to the postsynaptic actin cytoskeleton via actin-binding and SH3 domain-containing proteins, such as cortactin (Du et al., 1998; Naisbitt et al., 1999) and Abp1 (Qualmann et al., 2004). Because the actin cytoskeleton plays a major role in organizing and shaping postsynaptic spines and thereby synaptic function, we first asked whether the F-actin binding ability of Abp1 plays a role in controlling the postsynaptic actin cytoskeleton and thereby in modulating spine morphology. We overexpressed the actin-binding domains of Abp1 (Fig. 1*A*) (Kessels et al., 2000) individually and in different combinations with the other domains of Abp1 in mature hippocampal neurons and analyzed spine morphology by quantitative measurements (Fig. 1*B–K*). Examinations of neurons transfected solely with GFP or mRFP used to outline neuronal morphology yielded identical spine shape parameters (data not shown) and were used for control purposes. All Abp1 constructs applied were approximately evenly distributed within the cytosol of transfected neurons (supplemental Fig. S1, available at www.jneurosci.org as supplemental material), i.e., they also reached peripheral dendrites and spines (magnified images in supplemental Fig. S1, available at www.jneurosci.org as supplemental material).

Transfection with full-length Abp1 highly significantly increased spine length (Fig. 1*C*) compared with control (Fig. 1*B*). Quantitative examinations of 500–1000 spines per group confirmed this finding and revealed an average length of spines of 1.56 ± 0.09 μm in Abp1-overexpressing cells compared with 1.30 ± 0.07 μm for control cells (Fig. 1*H–K*). The effect was also observed during overexpression of an Abp1 ΔSH3 deletion mutant. Also deletion of the flexible domain, the binding site for Src family kinases (Larbolette et al., 1999), did not abolish the increased spine length effect. The two independent, N-terminal actin-binding domains of Abp1 were sufficient to increase spine length and even the individual domains were able to elongate spines (Fig. 1*F–H*,*K*). Cumu-

lative analyses (Fig. 1*K*) showed that the effects of overexpression of full-length Abp1 differed from those of all other Abp1 constructs encompassing the actin-binding modules. The full-length graph displayed a strong convergence toward the control curve above spine sizes of 1.5 μm and, very similar to control, reached a plateau at 2.5 μm. In contrast, in neurons overexpressing the other Abp1 constructs, ~20% of the spines were 2.5 μm in length and longer (Fig. 1*K*).

We next analyzed all four established spine morphology groups (i.e., filopodia and thin spines, stubby spines, branched spines, and mushroom spines) (for examples, see Fig. 2*A–D*) individually. The two major groups of postsynaptic spines, thin spines and filopodia and mushroom spines, showed marked differences in their appearance during overexpression of Abp1 deletion mutants compared with full-length Abp1 (Fig. 2*E–H*). The length of thin spines and filopodia in full-length Abp1-overexpressing cells was similar to control, whereas the Abp1 deletion mutants tested led to significant length increases (Fig. 2*E*,*F*).

In contrast, the length of mushroom spines was also highly significantly increased by overexpression of full-length Abp1 (Fig. 2*G*,*H*). As best seen in the cumulative analyses (Fig. 2*H*), a significant portion of mushroom spines was ~2 μm long, and some spines of this class were even longer. This increase could be attributed to a selective lengthening of the spine neck, because the head shapes were unchanged (compare also Fig. 1*I*,*J* and quantitative analysis presented in Fig. 6). Because such elongated spines were virtually absent in control cells (Fig. 2*H*), we asked whether these altered postsynaptic structures contain a postsynaptic apparatus and are contacted by presynapses. Immunofluorescence analyses with antibodies against Piccolo (Fig. 2*I–K*), a prominent protein of the presynaptic active zone, and with antibodies against the postsynaptic scaffold proteins ProSAP1/Shank2 (Fig. 2*L–N*) and PSD-95/SAP90 (data not shown) revealed that elongated spines induced during overexpression of Abp1 contain postsynaptic components and are in contact with presynapses.

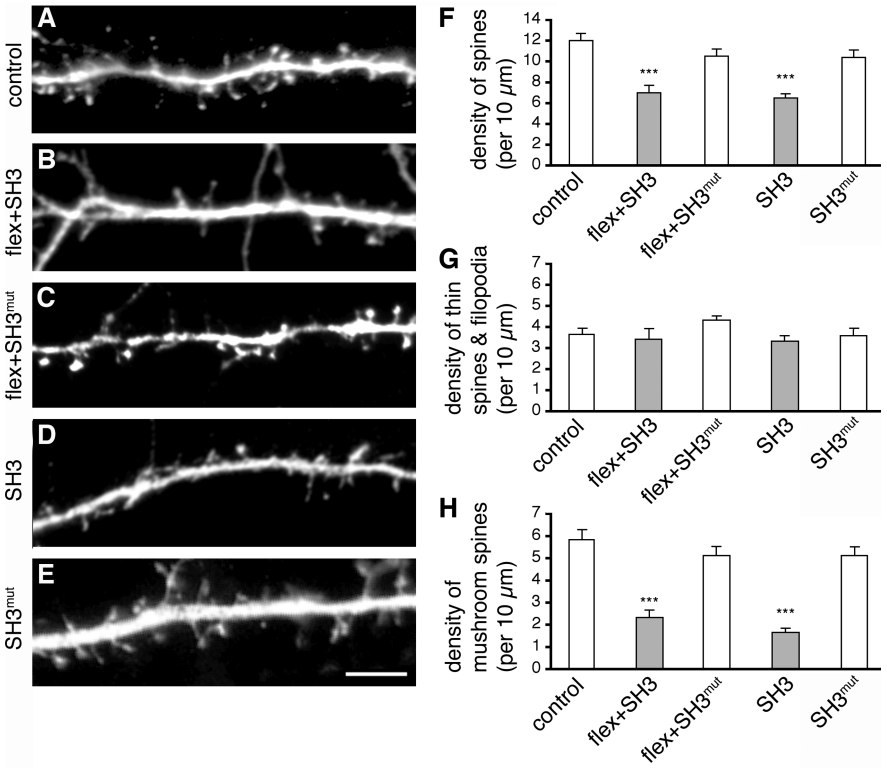

Figure 4. Overexpression of Abp1 fragments encompassing the C-terminal SH3 domain highly significantly decreases the density of mushroom spines. ***A–E***, Images show changes in spine density of hippocampal neurons at 14 DIV transfected at 12 DIV with C-terminal Abp1 fragments and mutants thereof. For neurons transfected with GFP as control (***A***) and cotransfected with GFP and myc-tagged Abp1 flex + SH3 (***B***), flex + SH3 ^{mut} (***C***), SH3 (***D***), as well as SH3 ^{mut} (***E***), GFP staining is shown, demonstrating the decrease in dendritic spine density triggered by C-terminal fragments of Abp1 including the wild-type SH3 domain. Scale bar, 5 μm. ***F–H***, Diagrams depict the means + SEM for the density of spines of all types (***F***) and their individual morphology groups (***G***, thin spines and filopodia; ***H***, mushroom spines) for neurons transfected with GFP alone (control) as well as cotransfected with C-terminal Abp1 fragments and mutants thereof as indicated. ***$p < 0.001$.

Abp1 promotes mushroom-type spine formation by molecular mechanisms dependent on both its F-actin binding and SH3 domain interactions

Besides the striking effects on spine length, we observed some increase in spine density in neurons with an excess of full-length Abp1 (Fig. 3*A*). Detailed quantitative analyses showed that there is no significant increase in the density of thin spines and filopodia (Fig. 3*B*). Spines with clearly recognizable heads, i.e., mushroom-type spines, however, are ~30% more abundant in Abp1-overexpressing neurons. This density increase was significantly different from control ($p < 0.05$) (Fig. 3*C*). Detailed quantitative analyses of the relative amount of all spine classes showed that Abp1 overexpression increases the abundance of mushroom spines at the expense of both thin spines and filopodia as well as stubby spines (Fig. 3*B–E*).

The fact that the mushroom spine density increase exclusively occurred with full-length Abp1 but that the actin-binding domains individually or in combination (ADF-H+helical) even have negative effects (Fig. 3*C*) suggested that the non-actin-binding C terminus is crucial for the promotion of mushroom spines observed during overexpression of full-length Abp1. Experiments with a deletion mutant solely lacking the C-terminal SH3 domain showed that it is not the flexible domain but the SH3 domain, which is crucial (Fig. 3*C*).

To examine the effect of Abp1 overexpression on synaptic organization further, we examined whether the observed increase in mushroom spine density corresponds to an increase in synapse formation. Anti-synapsin staining indeed suggested that this was the case (Fig. 3*F*,*G*). Quantitation of synapsin-positive puncta at Abp1-overexpressing neurons indeed showed a clear increase in synapse formation (Fig. 3*H*). The increase in synapse number was even stronger than that of morphologically identified mushroom spines. This underestimation of Abp1-induced synapse formation by analyses of spine shape is most likely attributable to the fact that some synapses, e. g. dendritic shaft synapses, do not have bulbous heads easily recognizable by morphometric analyses.

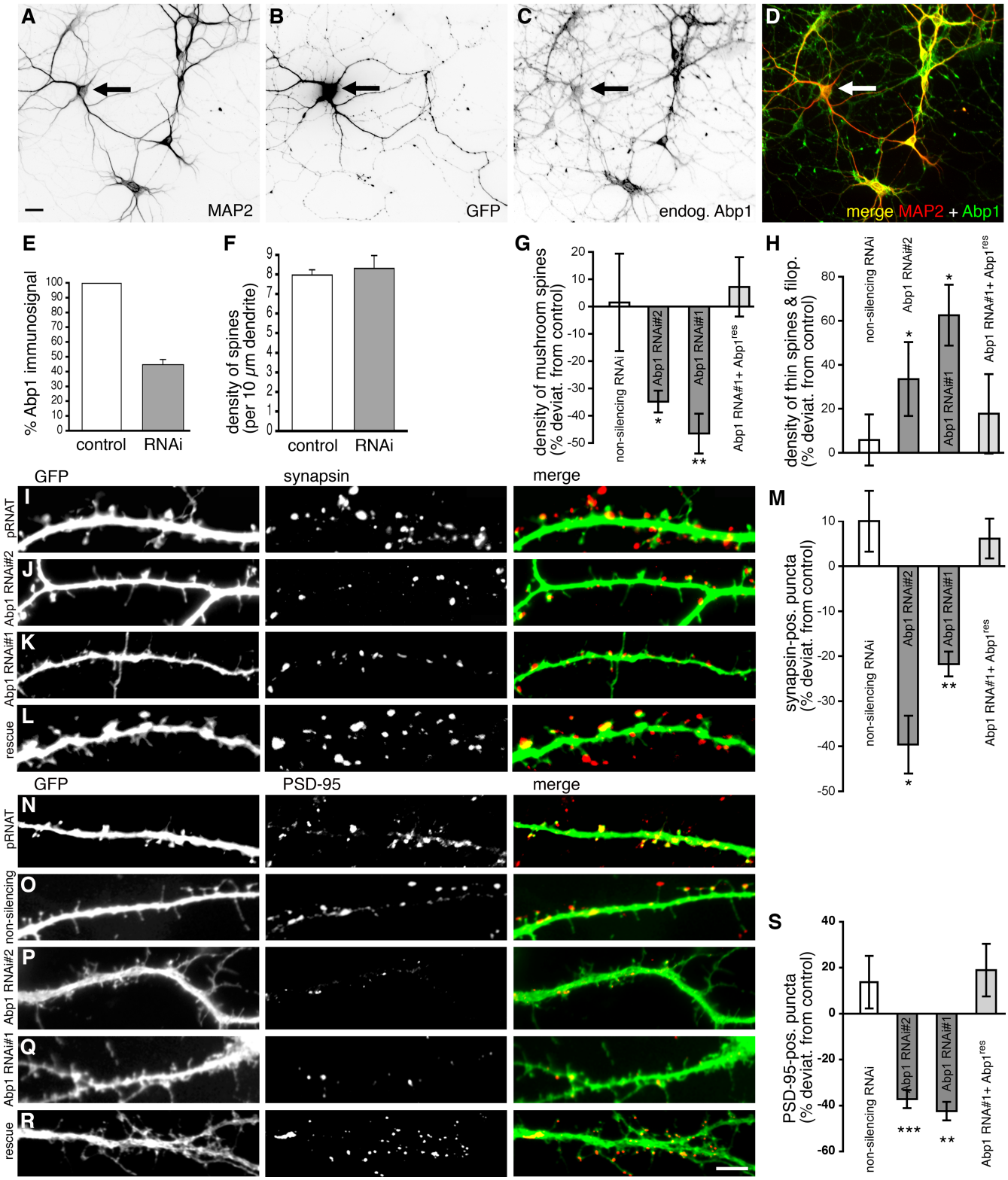

Figure 5. RNAi-based reduction of Abp1 expression levels reduces the densities of mushroom spines and synapses on hippocampal neurons. ***A–D***, Primary hippocampal neurons were transfected at day 12 in culture with a vector encoding for GFP and small interfering RNAs complementary to the Abp1 message under two different promotors. Neuronal cells were identified by anti-MAP2 immunostaining [***A***; depicted in red (false color) in the merged image ***D***]. Neurons transfected with the pRNAT-driven Abp1 RNAi construct are marked by GFP expression (arrow; ***B***) and showed a significant reduction in the anti-Abp1 immunoreactivity [***C***; shown in green (false color) in the merged image ***D***]. ***E***, Quantitative analysis of the anti-Abp1 immunoreactivity of 21 neurons transfected with a pRNAT-driven Abp1 RNAi construct (marked by GFP coexpression) demonstrates that Abp1 RNAi results in ~56% reduction of the anti-Abp1 immunofluorescence intensity when compared with untransfected neurons ($n = 77$). The intensity of fluorescence was measured in the bodies of all MAP2-positive cells. Data are represented as mean + SEM. ***A–F*** represent data for Abp1 RNAi sequence 1 (Abp1 RNAi sequence 2 gave similar results). ***F–S***, Analyses of the effects of knocking down Abp1 on spine morphology and synapse density. Primary hippocampal neurons were transfected with pRNAT–GFP (control), a nonsilencing RNAi construct, pRNAT-driven Abp1 RNAi sequences 1 and 2 and double-transfected with Abp1 RNAi sequence 1, and an RNAi-resistant but otherwise unaltered Abp1 mutant (Abp1 RNAi#1 + Abp1^{res}, rescue), respectively, at 12 DIV and fixed after 48 h. Diagrams show that the density of spines of all types (means + SEM) (***F***) is unchanged but that the densities of spines of individual morphology groups (***G***, mushroom-shaped spines; ***H***, thin spines and filopodia in percentage deviation ± (*Figure legend continues*.)

The SH3 domain of Abp1 has a dominant-negative effect on spine density and mushroom spine formation

To address the issue whether the SH3 domain is not only crucial but maybe also sufficient for the observed spine density increase, we used two different C-terminal Abp1 constructs, the entire C-terminal half of the protein, i.e., a construct only lacking the two actin-binding domains (flex+SH3), and the SH3 domain alone (Fig. 4). Both Abp1 deletion mutants were expressible in primary neurons. Immunosignals were strongest in the cell bodies, but additionally a distribution into peripheral dendrites and postsynaptic spines was observed (supplemental Fig. S2, available at www.jneurosci.org as supplemental material). The excess of both Abp1 deletion mutants led to a prominent decrease in spine density (Fig. 4*B*,*D*) when compared with either control (Fig. 4*A*) or overexpression of corresponding constructs carrying two point mutations within the SH3 domain (Fig. 4*C*,*E*). These mutations disrupt classical SH3 domain/PXXP-motif interactions (Kessels et al., 2001). Quantitative examinations of mushroom spines showed that the effects of the C-terminal half of Abp1 and of the isolated SH3 domain were comparable. Overexpression of both constructs led to a highly significant decrease in spine density (Fig. 4*F*) ($p < 0.001$).

Quantitative analyses of the different spine classes showed that there was no effect on thin spines and filopodia at all (Fig. 4*G*), whereas the number of mushroom-shaped spines was strongly reduced. Both the combination of flexible and SH3 domain as well as the SH3 domain alone caused spine densities to drop to approximately one-third of that of control and the two different mutants including a nonfunctional SH3 domain ($SH3^{mut}$ and $flex+SH3^{mut}$), respectively (Fig. 4*H*).

Our observations that overexpression of full-length Abp1 led to an increased number of mushroom spines and that an excess of either the actin-binding domains of Abp1 or the C-terminal SH3 domain had strong negative effects on mushroom spine density strongly suggest that the Abp1 SH3 domain is crucial but by itself not sufficient for mushroom spine formation. Instead, a combination of SH3 domain interactions and F-actin binding by Abp1 is required to promote mushroom spines.

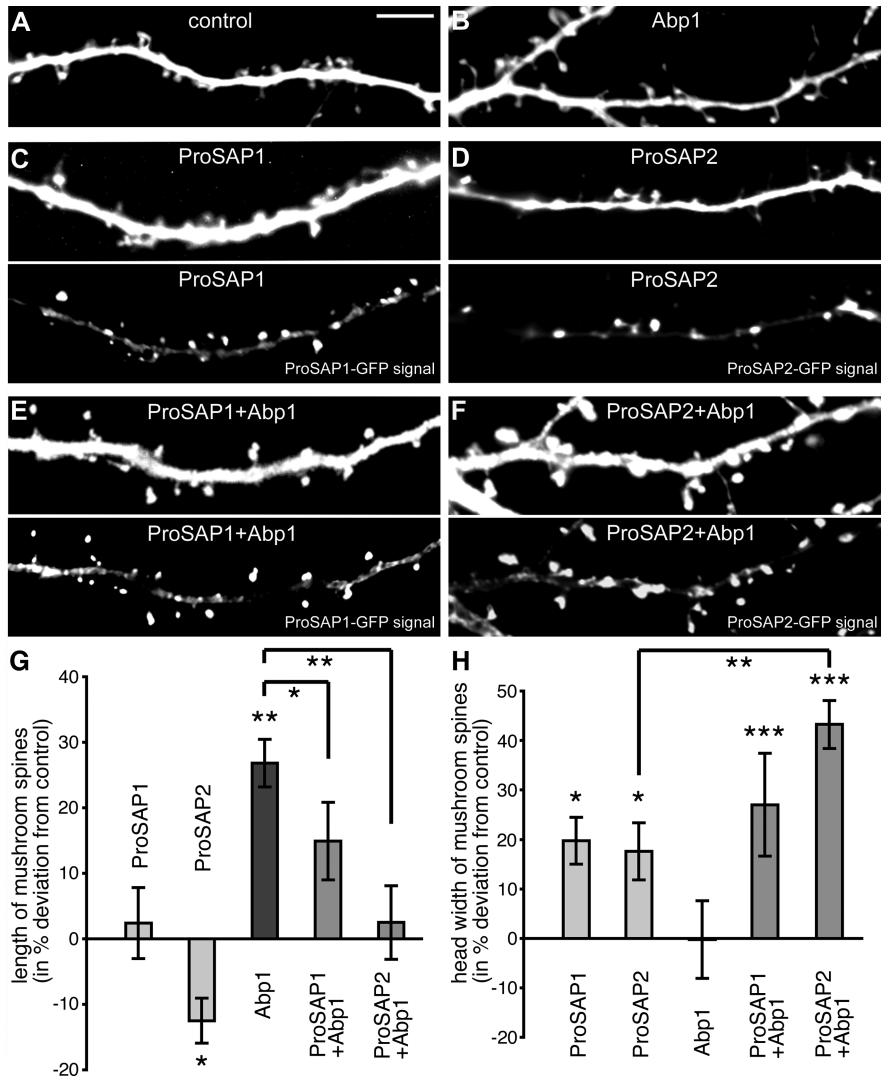

Figure 6. The physical interaction partners Abp1 and ProSAPs/Shanks cooperate in controlling mushroom-type spine morphology. ***A–F***, Images show enlarged heads of mushroom-shaped spines of primary hippocampal neurons at 14 DIV during overexpression of ProSAP1 (***C***) and ProSAP2 (***D***) compared with spine heads of mRFP-expressing cells (control, ***A***) and Abp1-expressing cells (***B***). Coexpression of ProSAP1+Abp1 (***E***) and ProSAP2+Abp1 (***F***), respectively, led to an additional promotion of ProSAP-induced head extension and to a decrease in Abp1-induced spine neck elongation. Images represent the fluorescence signals of cell-filling molecules cotransfected to highlight the morphology. Bottom rows in ***C–F*** show the fluorescence signals of GFP–ProSAP1 and GFP–ProSAP2. ***G***, ***H***, Diagrams depict the means ± SEM for the length of mushroom spines (***G***) and the head width of mushroom spines (***H***) in percentage deviation from mRFP-transfected control cells for neurons expressing ProSAP1, ProSAP2, Abp1, or combinations thereof as indicated. *$p < 0.05$; **$p < 0.01$; ***$p < 0.001$. Scale bar, 5 μm.

Abp1 knockdown reduces mushroom spines and synaptic contacts

To address whether Abp1 is not only involved in the formation of mushroom spines but is also crucial for this process, we generated three different vector-based RNAi tools against rat Abp1 that additionally express GFP as a reporter, transfected primary hippocampal neurons with these bicistronic constructs, and tested GFP-positive neurons, as identified by anti-MAP2 staining (Fig. 5*A*,*B*), for their content of endogenous Abp1 by anti-Abp1 immunostaining (Fig. 5*C*). With two of the RNAi tools we gener-

←

(*Figure legend continued.*) SEM from pRNAT-expressing, i.e., GFP-expressing, control cells) are significantly different in Abp1-deficient cells. Whereas immature thin spines and filopodia prevail, mushroom spine density is strongly decreased. ***I–S***, Analyses of synapse density based on immunostaining of the presynaptic marker synapsin (***I–M***) and based on immunostaining of the postsynaptic marker PSD-95 for synapse detection (***N–S***), respectively, reveal reduced numbers (means ± SEM) of PSD-95-positive (***S***) and synapsin-positive (***M***) puncta on dendrites from neurons expressing Abp1 RNAi compared with different sorts of control neurons. Note that restoration of Abp1 levels by cotransfection of an RNAi-resistant Abp1 mutant rescues the reduction of synapses as well as the defects in mushroom spine morphology control. *$p < 0.05$, **$p < 0.01$, ***$p < 0.001$. Scale bars: (in ***A***) ***A–D***, 20 μm; (in ***R***) ***I–L***, ***N–R***, 5 μm.

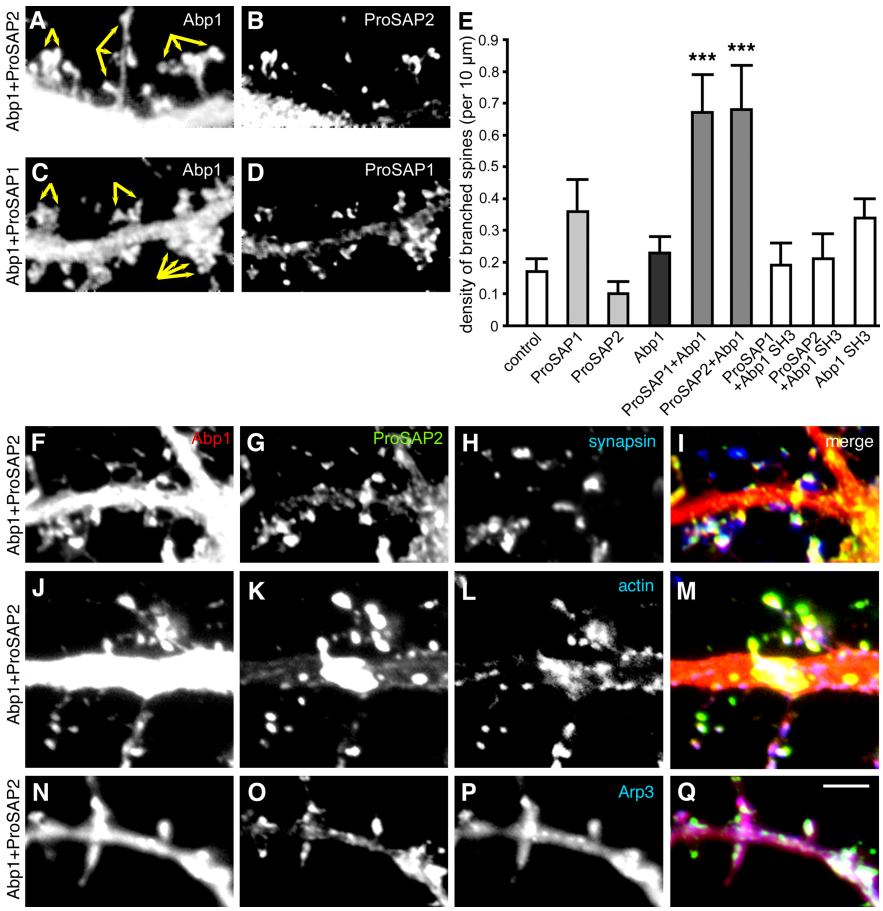

Figure 7. Abp1 and ProSAP1 or ProSAP2 coexpression leads to highly branched and complex spines with multiple enlarged spine heads. ***A–D***, Coexpression of Abp1 (***A***, ***C***) with ProSAP2 (***B***) and ProSAP1 (***D***), respectively, results in highly branched spines with cauliflower- or broccoli-like appearance in primary hippocampal neurons at 14 DIV (examples marked by arrows). ***E***, Quantitative analysis of the density of branched spines, depicted are the means + SEM, reveals that cooverexpression of Abp1 with ProSAP1 as well as with ProSAP2, but not expression of the individual proteins, leads to a highly significant increase in irregular, branched, multi-headed spines compared with control cells transfected with the cell-filling molecule RFP. In contrast, coexpression of the isolated SH3 domain of Abp1 with ProSAPs was not sufficient for the induction of these highly branched and complex spines with multiple enlarged heads. ***$p < 0.001$. ***F–Q***, Enlarged spines induced by coexpression of Abp1 (***F***, ***J***, ***N***; red in merged images ***I***, ***M***, ***Q***) and ProSAP2 (***G***, ***K***, ***O***; green in merged images ***I***, ***M***, ***Q***) are aligned with presynaptic structures marked by synapsin immunoreactivity (***H***; blue in merged image ***I***), are marked by high content of F-actin stained with phalloidin (***L***; blue in merged image ***M***), and also contain immunoreactivity for the actin nucleation machinery Arp2/3 complex (anti-Arp3, ***P***; blue in merged image ***Q***). Colocalization of Abp1 and ProSAP2 with synapsin, F-actin, and Arp3, respectively, appears white in the merged images. Scale bar (in ***Q***): ***A–D***, ***F–Q***, 5 μm.

ated, a significant reduction of the anti-Abp1 signal in transfected neurons was obtained (Fig. 5*A–D*). Quantitative evaluations showed that, during overexpression of RNAi sequence 1, the Abp1 signal is reduced to <38% compared with pRNAT-transfected primary neurons (data not shown) and to <44% compared with untransfected primary neurons (Fig. 5*E*). RNAi sequence 2 yielded similar results (data not shown).

A quantitative evaluation of the density of all spiny structures in neurons with reduced Abp1 content did not yield any differences compared with the pRNAT control (Fig. 5*F*). Likewise, the length of spines was unaffected (data not shown).

Detailed analyses of the morphological properties of the spines formed during acute reduction of Abp1 expression levels, however, revealed that Abp1 is a crucial component in the formation of mature, mushroom-type spines. Mushroom spine density showed a reduction of 46.54 ± 7.31 and 34.85 ± 3.99% compared with control cells in primary hippocampal neurons transfected with RNAi sequences 1 and 2, respectively (Fig. 5*G*), whereas thin spine density is correspondingly increased (to 135–162% of the control value) (Fig. 5*H*). Importantly, the two different RNAi sequences yielded consistent results. Coexpression of an RNAi-resistant but otherwise unaltered Abp1 mutant (rescue) (Fig. 5) rescued both of the observed defects. Both the mushroom spine density decrease and the increase of thin spines were abolished, and the densities equaled approximately control levels (Fig. 5*G*,*H*). Together, this firmly proves the specificity of the RNAi approach.

The effect of Abp1 knockdown mirrors the reduction in mushroom spine density observed during overexpression of either the isolated SH3 domain (Fig. 4*H*) or the actin-binding modules of Abp1 (Fig. 3*C*), which both seem to act in a dominant-negative manner. Furthermore, it can be concluded that Abp1 knockdown has an effect opposite to the gain-of-function manipulation, the overexpression of wild-type full-length Abp1 (Fig. 3*C*).

The decrease in mushroom spine abundance during Abp1 RNAi corresponded with a pronounced reduction in the number of synaptic structures. Both the number of contacting presynaptic structures (identified as synapsin-positive puncta) (Fig. 5*I–M*) and the number of postsynapses (identified as PSD-95-positive puncta) (Fig. 5*N–S*) were diminished by ~40% in neurons with reduced Abp1 expression (Fig. 5*J*,*K*,*P*,*Q*) compared with neurons expressing pRNAT–GFP (control) (Fig. 5*I*,*N*) and a nonsilencing RNAi construct (Fig. 5*O*), respectively. Again, the two different RNAi sequences led to consistent effects. The specificity of this Abp1 RNAi effect is also demonstrated by experiments, in which we restored Abp1 expression levels by cotransfection of an RNAi-resistant Abp1 mutant. Cotransfection of this Abp1 mutant with Abp1 RNAi sequence 1 completely abolished the highly significant reduction of synapsin-positive and PSD-95-positive structures observed in RNAi-transfected neurons (Fig. 5*L*,*R*). The quantitative values obtained in such rescue experiments were not significantly different from the two control incubations, pRNAT and nonsilencing RNAi, respectively (Fig. 5*M*,*S*).

The negative Abp1 loss-of-function effect on synapse density is consistent with Abp1 overexpression showing the opposite effect, i.e., a highly significant increase in synapse density (Fig. 3*H*).

Abp1 and ProSAP/Shanks cooperate in mushroom spine morphology control

In the postsynaptic compartment, Abp1 associates via its SH3 domain directly with members of the ProSAP/Shank protein family (Qualmann et al., 2004), important scaffolding proteins in the PSD. This suggests that the cytoskeletal component Abp1 may cooperate with ProSAP/Shank proteins in regulating spine morphology. Indeed, we observed that the highly significant in-

crease of the length of mushroom spines (compare also Fig. 2) is quenched by cooverexpression of the Abp1 binding partners ProSAP1 (Shank2) and ProSAP2 (Shank3), respectively (Fig. 6*B–G*). The increase in mushroom spine length during Abp1 overexpression, to which both actin-binding modules (Fig. 2) of Abp1 contribute, is thus counterbalanced by a corresponding increase in ProSAP expression levels, indicating that a tight balance of Abp1 and its postsynaptic interaction partners is important for proper spine development.

Shank1 has been reported to induce an enlargement of spine heads when overexpressed in primary hippocampal neurons (Sala et al., 2001). Our analyses show that also ProSAP1/Shank2 and ProSAP2/Shank3 have effects on spine head extension. Quantitative measurements revealed that the average width of spine heads is increased by ~20% during overexpression of ProSAP1 and ProSAP2, respectively (Fig. 6*C*,*D*,*H*).

To reveal any cooperative effects of Abp1 with ProSAPs in the control of mushroom spine head size, control, wild-type full-length Abp1, which during single expression has no effect on head width of mushroom-shaped spines (Fig. 6*B*,*H*), was coexpressed with both ProSAP1 (Fig. 6*E*) and ProSAP2 (Fig. 6*F*). As clearly visible from the images (Fig. 6*E*,*F*) and quantitatively confirmed by evaluating >300 mushroom-type spines per group, Abp1 coexpression resulted in an additional and highly significant increase in the head width of mushroom spines (Fig. 6*H*) (see also Fig. 10*J*). Because neither ProSAP expression levels are increased nor the localization of ProSAPs is affected by Abp1 coexpression, these data indicate that the cytoskeletal component Abp1 cooperates with the ProSAP/Shank family in controlling spine morphology.

This conclusion is further strengthened by our observation that Abp1 and ProSAPs only in combination but not individually promote the formation of irregular, branched, multi-headed spines. Cooverexpression of Abp1 with ProSAP1/Shank2 or ProSAP2/Shank3 led to a highly significant, ~400% increase of irregular, branched structures, which often appeared as huge multi-headed spine aggregates (Fig. 7*A–D*) and were extremely rare in control conditions (Fig. 7*E*). Furthermore, the few branched structures found in controls were mostly thin branched spines, which usually do not even have heads, whereas in cells cooverexpressing ProSAPs and Abp1, the structures counted as branched spines were much larger and multi-headed.

Interestingly, cotransfection of the Abp1 SH3 domain instead of the full-length protein failed to elicit this Abp1–ProSAP-mediated effect. Because expression of the SH3 domain alone has no negative effect, this suggests that the actin binding properties of Abp1 are required and functionally contribute to the induction of multiple spine heads (Fig. 7*E*).

The extended spines induced by Abp1 and ProSAP overexpression were positive for Abp1, for ProSAPs, for additional postsynaptic markers, such as the NMDA receptor subunit 2B (data not shown), for presynaptic markers, such as synapsin (Fig. 7*F–I*), for F-actin (Fig. 7*J–M*), and for the actin nucleation machinery Arp2/3 complex (Fig. 7*N–Q*).

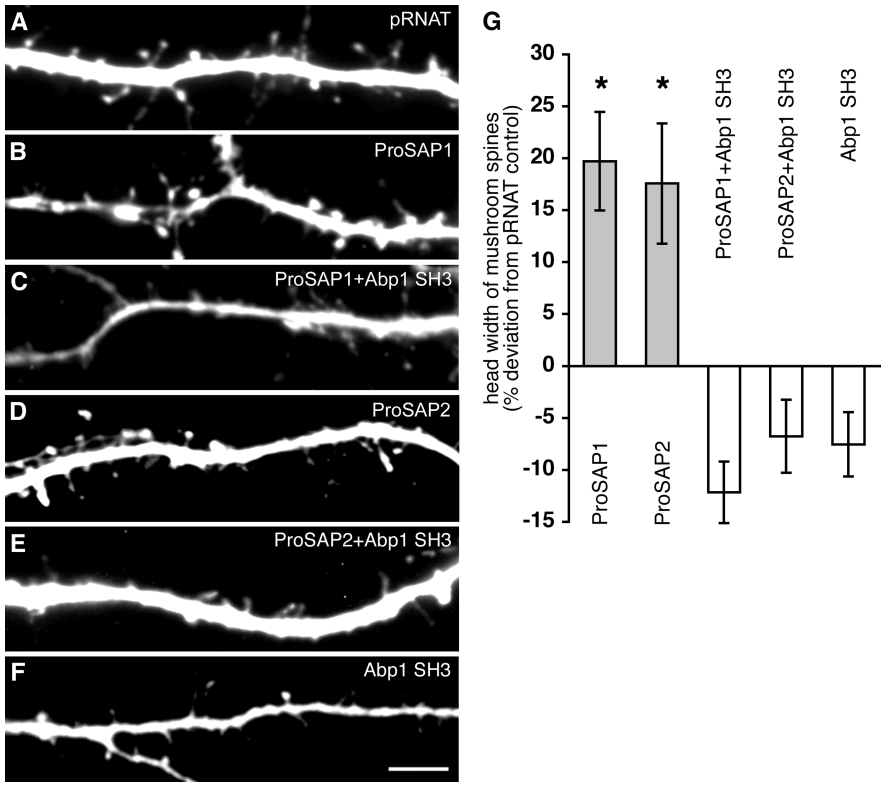

Figure 8. Abp1–ProSAP complex formation is crucial for ProSAP-induced enlargements of spine heads. ***A–F***, Images of spine morphology of primary hippocampal neurons at 14 DIV expressing a cell-filling molecule alone (***A***, pRNAT-driven GFP expression) and of cells cotransfected with ProSAP1 (***B***), ProSAP1+Abp1 SH3 (***C***), ProSAP2 (***D***), ProSAP2+Abp1 SH3 (***E***), and the Abp1 SH3 domain (***F***), respectively. Images show the fluorescence channel for the cell-filling molecule to highlight cell morphology. ***G***, Quantitative analysis of head widths of mushroom spines reveals that the increase in head width of mushroom spines [depicted are the means ± SEM in percentage deviation from control (cells transfected with GFP-expressing pRNAT vector)] for neurons expressing ProSAP1 and ProSAP2 is abolished during cotransfection of the isolated Abp1 SH3 domain. $*p < 0.05$. Scale bar, 5 μm.

ProSAP/Shank-induced enlargements of spine heads in mushroom spines are critically dependent on SH3 domain-mediated complex formation with Abp1

Our analyses have revealed that Abp1 cooverexpression can potentiate the ProSAP-induced enlargements of spine heads and is involved in the formation of ectopic spine heads from mushroom spines. We thus next asked whether interfering with the ProSAP–Abp1 interaction would cause any effects on the ProSAP/Shank-induced head enlargement process. For this purpose, we used the isolated ProSAP-binding interface, the SH3 domain of Abp1, as a putative blocking tool (Fig. 8). Both visual inspection (Fig. 8*A–F*) and the confirmation by quantitative analyses revealed that the increase in head width of mushroom spines of neurons expressing ProSAP1 (Fig. 8*B*,*G*) and ProSAP2 (Fig. 8*D*,*G*) is completely abolished during cotransfection of the isolated Abp1 SH3 domain (Fig. 8*C*,*E–G*).

ProSAP-mediated spine enlargements depend on the Arp2/3 complex, its activator N-WASP, and Abp1

The enlarged spine structures induced during ProSAP1 and ProSAP2 overexpression are marked by accumulation of filamentous actin and of the actin nucleator Arp2/3 complex (Fig. 7*J–Q*). We

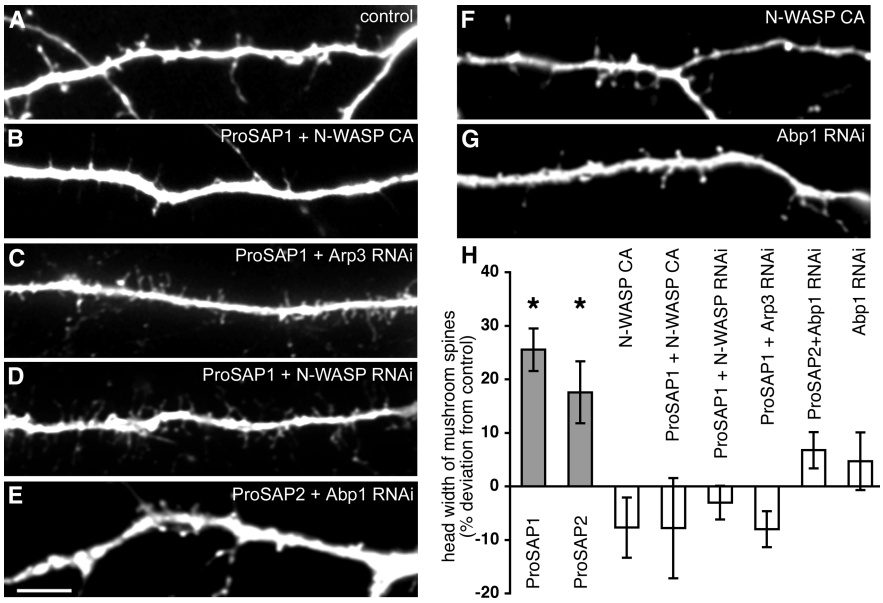

Figure 9. Arp2/3 complex activation, the Arp2/3 complex activator N-WASP, and the N-WASP-controlling and ProSAP-binding protein Abp1 are crucial for ProSAP-induced enlargements of spine heads. ***A–G***, Images of spine morphology of primary hippocampal neurons at 14 DIV expressing a cell-filling molecule alone (***A***) and of cells cotransfected with ProSAP1 + N-WASP CA (***B***), ProSAP1 + Arp3 RNAi (***C***), ProSAP1 + N-WASP RNAi (***D***), and ProSAP2 + Abp1 RNAi (***E***), as well as with N-WASP CA (***F***) and Abp1 RNAi alone (***G***), respectively. Cell morphologies shown represent the fluorescence signals for the cell-filling molecules used. For examples of enlarged spines observed during expression of ProSAP1 and ProSAP2, respectively, see Figure 8, *B* and *D*. ***H***, Quantitative analysis of head widths of mushroom spines (means ± SEM in percentage deviation from control) show that ProSAP1- and ProSAP2-induced head enlargements are dependent on Arp2/3 complex activity and sufficient supplies of Arp3, N-WASP, and Abp1. $*p < 0.05$. Scale bar, 5 μm.

thus asked whether ProSAPs induce spine head enlargements via promotion of local formation of actin filaments (Fig. 9*A–H*). Coexpression of the Arp2/3 complex inhibitory N-WASP CA (Strasser et al., 2004; Pinyol et al., 2007) indeed prevented ProSAP-mediated head enlargements, and spines were indistinguishable from control (Fig. 9*A*,*B*,*F*,*H*). That this suppression of ProSAP functions was indeed attributable to a specific lack of Arp2/3 complex function was demonstrated by the fact that coexpression of an Arp3 RNAi plasmid (Pinyol et al., 2007) caused a similar suppression of ProSAP-induced spine morphology changes (Fig. 9*C*,*H*).

These data suggested that the ProSAP-induced spine phenotype requires new actin filament polymerization by the actin nucleator Arp2/3 complex, which Abp1 is able to steer via N-WASP activation (Pinyol et al., 2007). We thus tested the effects of knocking down N-WASP. Indeed, ProSAP-mediated spine head enlargement was also suppressed by RNAi-mediated N-WASP deficiency (Fig. 9*D*,*H*).

To explicitly address whether Abp1 is crucial for ProSAP-mediated spine morphology control, we expressed Abp1 RNAi plasmids together with ProSAP2 (Fig. 9*E*). Reduction of Abp1 expression levels indeed led to an almost complete suppression of ProSAP effects (Fig. 9*H*).

Our experiments thus demonstrate that Abp1 is crucial for ProSAP/Shank functions and suggest that Abp1–ProSAP complex formation via the Abp1 SH3 domain is an underlying molecular mechanism.

A ProSAP1 mutant lacking all Abp1 binding sites is unable to induce spine head enlargement

We have demonstrated that Abp1 is crucial for spine head and synapse formation. Both its SH3 domain and functions of the N-terminal F-actin binding modules seem important, because the SH3 domain alone has a dominant-negative effect. Also, we were able to demonstrate that Abp1 is crucial for the effects mediated by its interaction partners ProSAPs and that ProSAP-mediated effects seem to specifically depend on Abp1–ProSAP complex formation. From these data, it can be hypothesized that a ProSAP mutant, which is incapable of binding Abp1, should be unable to elicit ProSAP-mediated spine head extension. To address this, we constructed a ProSAP1 mutant, in which two prolines of the deduced Abp1 SH3 domain-binding proline-rich motif (Qualmann et al., 2004) in the ProSAP1 C terminus were exchanged for alanine (ProSAP1 PP950/1AA). Surprisingly, this mutant still associated with the Abp1 SH3 domain (Fig. 10*A*), suggesting that there may be additional, thus far unknown, Abp1 binding sites within the ProSAP1 molecule. This conclusion was confirmed by testing several pieces of ProSAP1 in coprecipitation experiments with the Abp1 SH3 domain (Fig. 10*B*). Similarly, ProSAP2 has a variety of independent Abp1 SH3 domain binding sites (our unpublished data).

In silico analyses of the sequences of ProSAP1 and ProSAP2 in conjunction with hints on Abp1 SH3 domain-binding preferences from peptide screening (Yamabhai and Kay, 1997) led to the prediction of at least five sites in ProSAP1. Among those, the deduced binding site from amino acids 946–957 (Qualmann et al., 2004), which we experimentally confirmed by both demonstrating that a peptide containing this site (ProSAP1 930–972) binds and that a C-terminal deletion mutant lacking the amino acids 946–957 (ProSAP1 528–1252 Δ946–957) does not bind to the Abp1 SH3 domain (Fig. 10*C*).

The more N-terminal part of ProSAP1 contains several binding sites, as deduced from testing a variety of additional deletion mutants (Fig. 10*C*,*D*). The very N terminus (amino acids 1–228) was deleted *en bloc* to generate a ProSAP1 mutant deficient for Abp1 binding because it encompasses several binding sites that precluded their individual deletion. Between amino acids 228 and 528, it was sufficient to delete the three following sites, amino acids 302–319, 407–414, and 519–527, to ensure lack of binding.

Overexpression of a ProSAP1 mutant lacking all Abp1 binding sites (ProSAP1$^{\Delta\text{Abp1 interf.}}$) in primary hippocampal neurons indeed failed to elicit spine head enlargement comparable with wild-type ProSAP1. Also, it did not show the strong cooperative effect with Abp1 on spine head extension observed for the wild-type protein. Instead, during expression of ProSAP1$^{\Delta\text{Abp1 interf.}}$ or its coexpression with Abp1, spine heads were indistinguishable from those observed in control cells (Fig. 10*E–J*).

Abp1-induced spine head and synapse formation is dependent on ProSAP2

Abp1 is crucial for spine morphology control and the formation of spine heads and synapses. We also clearly demonstrated that ProSAP-mediated spine head extension is dependent on Abp1 and on the SH3 domain/poly-proline motif-mediated Abp1/ProSAP complex formation and that both components act to-

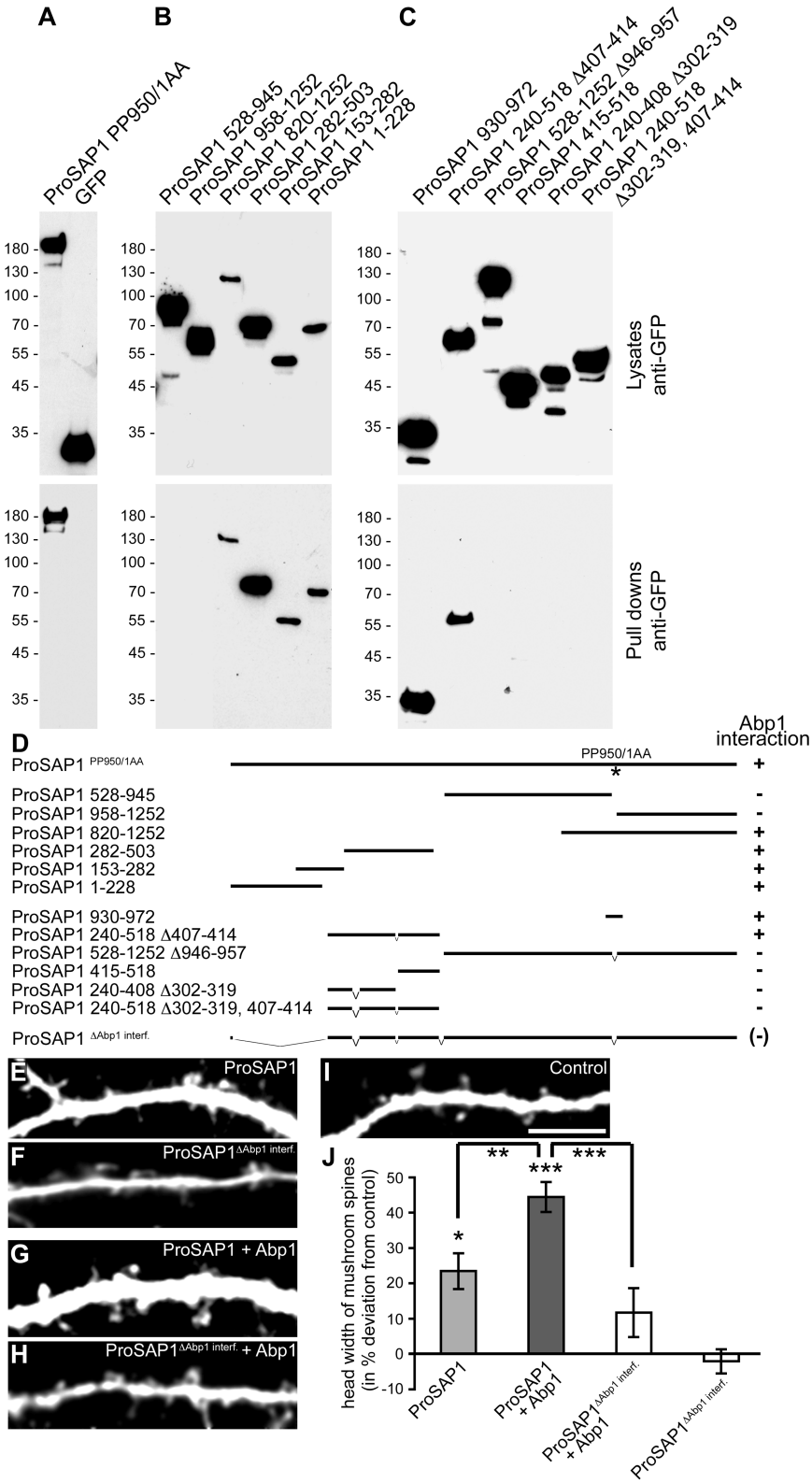

Figure 10. A ProSAP1 mutant lacking all the Abp1 binding sites fails to elicit spine head enlargement when overexpressed alone or in combination with Abp1. ***A–C***, Affinity purifications of ProSAP1 GFP-fusion proteins expressed in HEK293 cells with immobilized GST–Abp1 SH3 domain. Top row shows the amount of GFP-fusion proteins offered in the pull-down experiments, and bottom row shows GFP-fusion proteins coprecipitated with GST–Abp1 SH3. Controls with immobilized GST were negative (data not shown). ***A***, ProSAP1 mutant PP950/1AA still specifically binds to the Abp1 SH3 domain. ***B***, Analyses of ProSAP1 pieces for Abp1 SH3 domain binding reveals the existence of several Abp1 binding sites. ***C***, Analyses of pieces and deletion mutants toward the identification and deletion of Abp1 binding sites. ***D***, Schematic depiction of ProSAP1 constructs used for the analyses shown in ***A–C***, of the ProSAP1 mutant with all Abp1 SH3 domain interfaces deleted (ProSAP1 $^{\Delta Abp1\ interf.}$) and of their Abp1 SH3 domain binding capability [+, Abp1 binding; −, no Abp1 binding; (−) concluded not to bind, because the pieces used to assemble this construct all fail to bind when tested individually]. ***E–I***, Images of spine morphology, as highlighted by coexpressed cell-filling molecules, of primary hippocampal neurons at 14 DIV expressing ProSAP1 (***E***), the ProSAP1 $^{\Delta Abp1\ interf.}$ mutant (***F***), ProSAP1 + Abp1 (***G***), and the ProSAP1 $^{\Delta Abp1\ interf.}$ mutant + Abp1 (***H***) compared with control cells overexpressing only cell-filling molecules (mRFP) (***I***). ***J***, Quantitative analysis of head widths of mushroom spines revealed that the ProSAP1 $^{\Delta Abp1\ interf.}$ mutant fails to increase spine heads both alone or in combination with Abp1. *$p < 0.05$; **$p < 0.01$; ***$p < 0.001$. Scale bar, 5 μm.

gether in head formation. To firmly experimentally demonstrate that Abp1-mediated effects on spine head and synapse formation depend on ProSAPs, we used RNAi-mediated knockdown of ProSAP2, which was established by Roussignol et al. (2005). Already knockdown (confirmed by anti-ProSAP2 immunostaining; data not shown) of one the two Abp1 binding partners of the ProSAP/Shank family had dramatic negative effects on the Abp1-induced increase in mushroom spine density (Fig. 11*A–D*) and synapse formation (Fig. 11*E–K*). Whereas Abp1 led to a pronounced increase in mushroom spine density and synapse number, (Fig. 11*A*,*D*,*E*,*F*,*K*; compare also Fig. 3), combination of Abp1 with ProSAP2 RNAi led to values indistinguishable from control (Fig. 11*B*,*D*,*G*,*H*,*K*). Thus, Abp1 executes its functions in synapse and spine head formation in close functional cooperation with ProSAPs.

Discussion

The cortical actin cytoskeleton, which underlies the entire plasma membrane, strongly determines cellular morphology and plasma membrane topology. Thereby, actin dynamics is crucial for induction and proper development of spines as well as for their maturation and changes in morphology (Matus, 2000; Schubert et al., 2006; Tada and Sheng, 2006). Such changes in the postsynaptic cytoskeleton, however, have to be tightly controlled by synaptic activity sensed by additional components of the PSD (Hering and Sheng, 2001).

We here reveal that the F-actin-binding protein Abp1 does not only interconnect the actin cytoskeleton with ProSAP/Shank proteins, major PSD scaffolding proteins linking different receptors and signaling components (Gundelfinger et al., 2006), but additionally serves as a cytoskeletal effector protein in spine morphogenesis. In line, previous studies revealed that Abp1 regulates Arp2/3 complex activity and thereby controls early neuronal development (Pinyol et al., 2007).

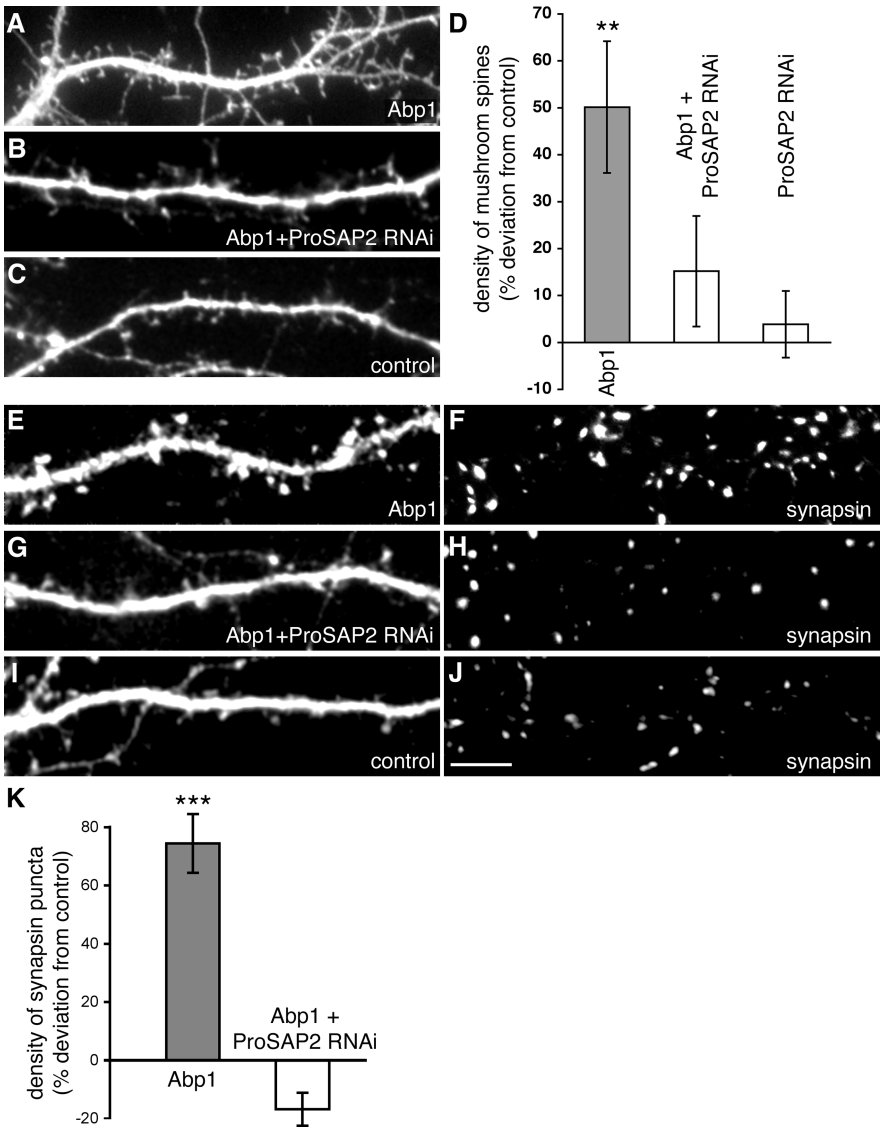

Figure 11. The Abp1-mediated increase in mushroom spine and synapse density is dependent on ProSAP2. ***A–C***, Images of spine morphology of primary hippocampal neurons at 14 DIV expressing Abp1 (***A***) and ProSAP2 RNAi + Abp1 (***B***) compared with control cells (***C***). ***D***, Quantitative analysis of mushroom spine density (means ± SEM in percentage deviation from control) shows that ProSAP2 RNAi effectively suppresses the Abp1-mediated increase in mushroom spine density. ***E–J***, Images of dendrites of Abp1 (***E***, ***F***), Abp1 + ProSAP2 RNAi (***G***, ***H***), and RFP-expressing cells (***I***, ***J***; control), contacting synapses of which were immunostained for the synaptic marker synapsin (***F***, ***H***, ***J***), show an increase of synapses on Abp1-overexpressing cells. ***A–C***, ***E***, ***G***, and ***I*** show the fluorescence channel for the cell-filling molecule to highlight cell morphology. ***K***, Quantitative analysis of synapse density as determined by counting synapsin puncta per 10 μm dendrite showed that the Abp1-mediated increase in synapses is completely suppressed by coexpression of ProSAP2 RNAi constructs (means ± SEM in percentage deviation from control). $^{**}p < 0.01$; $^{***}p < 0.001$. Scale bar, 5 μm.

In vitro, Abp1 uses two distinct N-terminal domains for F-actin binding (Kessels et al., 2000). Our analyses show that both domains individually as well as in combination localize to postsynaptic spines and have the capability to modulate spine shape by increasing the length regardless of spine type. These data for the first time show that F-actin binding by Abp1 modulates the actin cytoskeleton in living cells. Because Abp1 associates with five actin monomers within filaments (Kessels et al., 2000), the observed spine elongations are very likely attributable to filament side binding and stabilization, i.e., promotion of the polymerized state of actin.

Actin binding of Abp1 alone, however, is unable to explain the crucial role of Abp1 in maturation of spines, which are characterized by a distinct head containing the PSD. Instead, promotion of head formation and extension clearly requires the Abp1 SH3 domain in conjunction with F-actin binding. In line with a coordinated role of these two functional parts of Abp1, an excess of the actin-binding domains has a strong negative impact on mushroom spine density. Such Abp1 deletion mutants will occupy places for endogenous Abp1 and other proteins with closely related functions, such as cortactin. As a consequence, Abp1 SH3 domain functions become uncoupled from actin binding.

The same phenotype, a strong decrease in mushroom-type spines, is caused by the SH3 domain-containing part of Abp1 lacking the actin-binding domains. This also argues for a coordinated role of both actin-binding and SH3 domain interactions. Consistently, also acute reduction of Abp1 levels by RNAi caused a reduction of mushroom spine and synapse density. Because Abp1 knockdown did not decrease total spine density but resulted in a selective decrease in mushroom-type spines with a concomitant increase in thin spines and filopodia, it can be concluded that Abp1 is critically involved in the maturation of spines and the development of spine heads. A reduction of spine head width upon Abp1 knockdown results in the loss of spines in the mushroom category and a corresponding increase in the category of thin spines, i.e., spines without discernable heads. Similar to the loss-of-function phenotype observed during Abp1 knockdown, reduction of the actin-binding protein cortactin also decreased the density of spines and synaptic structures (Hering and Sheng, 2003).

What exactly may be the crucial role of Abp1 in spine head formation? We have shown that Abp1 directly binds ProSAP1/Shank2 and ProSAP2/Shank3 via its SH3 domain and can simultaneously associate with dynamic, newly formed actin filaments (Qualmann et al., 2004). Interestingly, a recent study revealed that ProSAP/Shanks do not just serve as platforms for organizing postsynaptic cytoskeletal functions but that also the maintenance of ProSAP/Shanks at the PSD, at least to some extent, is affected by disrupting actin filaments by incubation with latrunculin A (Kuriu et al., 2006). The fact that the Abp1 SH3 domain alone has a strong negative impact on mushroom spine density but in the full-length context, i.e., in combination with the F-actin-binding ability of Abp1, specifically promotes the formation of mushroom-type spines, suggests that one function of Abp1 in establishing spine heads is to interconnect ProSAP/Shank proteins with dynamic F-actin (Fig. 12).

In line with this, Rostaing et al. (2006) demonstrated by quantitative immunoelectron microscopy and tomography that the localization domains of ProSAP/Shanks and F-actin overlap at

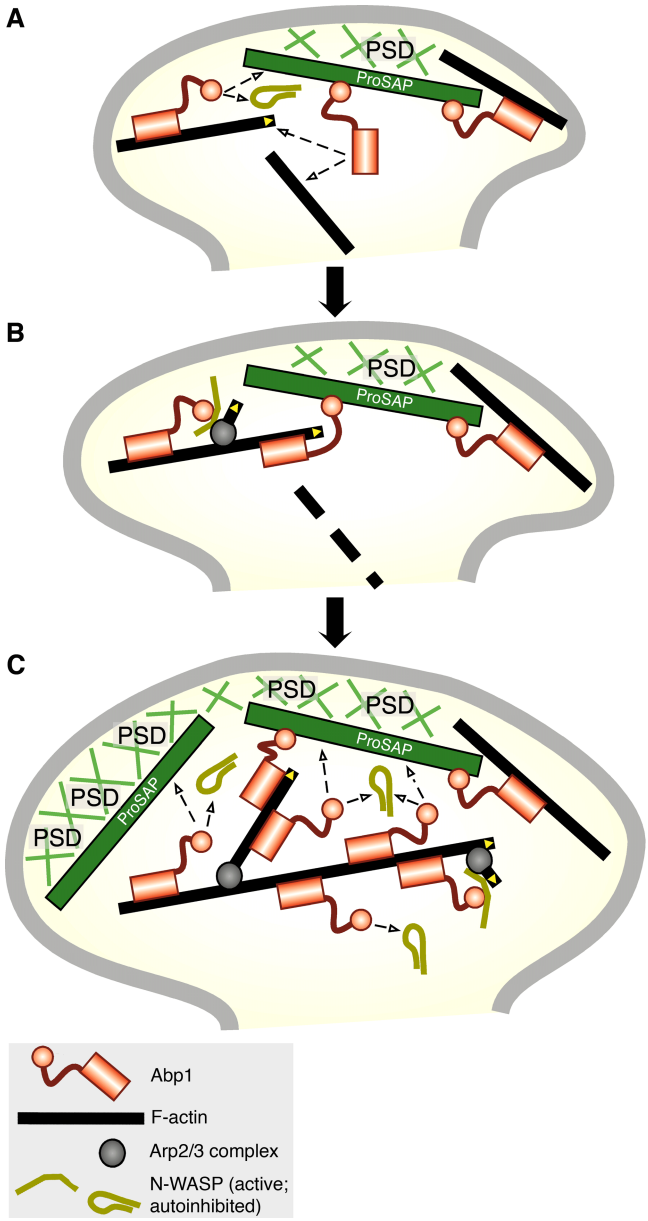

Figure 12. Model of the Abp1 functions in spine morphology control and synapse formation. ***A***, ProSAP molecules incorporated at sites of forming synapses allow for recruitment of Abp1 molecules in addition to those molecules interacting with dynamic F-actin at the cell cortex. Abp1 can interconnect ProSAPs with dynamic actin filaments contributing to the stability and growth of a ProSAP-attached actin cytoskeleton. Newly polymerizing actin filaments stabilized in the vicinity of ProSAPs efficiently recruit more Abp1 molecules, which may stabilize these actin filaments by side binding (***A***), whereas unbound filaments may show a higher sensitivity for depolymerization (***B***). Because ProSAPs seem to be the minimum factor in Abp1–ProSAP complex formation, as an excess of ProSAPs efficiently uses the pool of endogenous Abp1 for at least some spine head enlargement whereas just providing more Abp1 without increasing the availability of ProSAPs has no effect, this F-actin-mediated recruitment of Abp1 to forming and/or extending postsynapses rapidly provides more binding sites for SH3 domain interaction partner than can be complexed with the limiting component in Abp1–ProSAP complex formation, ProSAP. This leads to a promotion of SH3 domain interactions with additional binding partners at postsynaptic sites. ***B***, Among these binding partners is N-WASP, a normally autoinhibited activator of the Arp2/3 complex actin nucleation machinery, which during Abp1 SH3 domain binding is brought into an open conformation able to activate the Arp2/3 complex. The result is strong *de novo* polymerization of actin filaments in the ProSAP- and Abp1-enriched spine head. ***C***, Enhanced actin filament formation and further recruitment of Abp1 and ProSAPs increases the spine head. In cells lacking sufficient Abp1, growth of spine heads is inhibited because of the lack of the Abp1-dependent transition from initial stages (***A***) to dynamic, extended postsynaptic structures (***C***). Under such condition, mature synaptic structures are thus not efficiently formed, and thin, immature spine structures without synaptic contact prevail.

the cytoplasmic surface of the PSD. Interestingly, reducing ProSAP2/Shank3 expression levels in hippocampal neurons led to a decrease in the density of spines with discernable necks and heads (Roussignol et al., 2005), i.e., to a phenotype similar to Abp1 knockdown.

In contrast to the situation in aspiny neurons, spine density in primary hippocampal neurons was not significantly increased during ProSAP/Shank overexpression (our unpublished observations). Also cooverexpression of Abp1 and ProSAPs failed to induce more spines (our unpublished observations). The observation that cooverexpression of Abp1 and ProSAP1 or ProSAP2 resulted in a highly significant increase in the density of highly branched and complex spines with multiple enlarged heads but expression of any of these proteins individually had no effects demonstrates the cooperative action of Abp1 and ProSAPs in spine head formation and morphology control.

Our results show that ProSAP/Shank-induced enlargement of spine heads, which was previously only described for Shank1 (Sala et al., 2001), is a general function of ProSAP/Shank proteins. The cooperativity of Abp1 and ProSAP1/Shank2 and ProSAP2/Shank3 in this process is highlighted by the fact that the Abp1-mediated increases of mushroom spine and synapse density are dependent on ProSAP2 and on complex formation with ProSAPs and that vice versa the spine head enlargements induced by ProSAP1/Shank2 and ProSAP2/Shank3 are dependent on Abp1. This latter relationship manifests in strong promotion of ProSAP effects by Abp1 coexpression and in a suppression of ProSAP effects by Abp1 RNAi. In line with the importance of Abp1–ProSAP complexes in spine head and synapse formation, overexpression of a ProSAP1 mutant lacking all the Abp1-binding sites failed to synergize with Abp1 in head extension. Also such a mutant did not lead to increased head widths when overexpressed alone.

In line with the molecular domains that mediate the Abp1–ProSAP interaction (Qualmann et al., 2004; this study), an excess of the isolated Abp1 domain responsible for the interaction, the SH3 domain, was sufficient to suppress ProSAP-mediated spine head enlargements. This can be explained by the properties of the isolated SH3 domain, which associates with ProSAPs (Qualmann et al., 2004; this study) but lacks the F-actin binding capability of Abp1 (Kessels et al., 2001). It thus prevents the formation of functional Abp1–ProSAP complexes.

Our observations suggest that the Abp1 SH3 domain is of special importance for formation and enlargement of spine heads and thus for formation of synapses. We have demonstrated recently that Abp1 does not only interconnect SH3 domain interaction partners including ProSAPs with a dynamic, newly polymerizing actin network but also has a crucial role in actin dynamics. Abp1 steers Arp2/3 complex-dependent actin nucleation by regulating Arp2/3 complex activators, such as N-WASP, via SH3 domain interactions, and thereby controls early neuronal morphology (Pinyol et al., 2007).

In spines, the capability of Abp1 to coordinate SH3 domain-mediated functions with dynamic actin filaments has the potential to serve as a powerful feedforward mechanism (Fig. 12). Abp1 is not only able to link dynamic actin fibers to ProSAP/Shank proteins and to stabilize actin filaments (Fig. 12*A*,*B*), but it is also able to link the SH3 domain interaction partners of the WASP superfamily of Arp2/3 complex activators with F-actin and to activate N-WASP. This leads to Abp1-controlled Arp2/3 complex-mediated nucleation of actin filaments in the microenvironment of the actin- and ProSAP/Shank-rich PSD. Formation of new actin filaments then provides even more Abp1 attachment

sides, because Abp1 prefers freshly polymerized actin filaments (Kessels et al., 2000). More F-actin-attached Abp1 then in turn means more SH3 domain interactions with Abp1 binding partners involved in PSD organization and actin polymerization and creates an elaborate actin network in spines, which has the power to expand the spine head (Fig. 12). In line with such a scenario, some Abp1 may be present in forming synapses but an accumulation of Abp1 in postsynapses was only observed at time points of neuronal development after the incorporation of the first pool of ProSAP/Shank molecules into forming postsynapses (Qualmann et al., 2004). Also, this model would explain why subsequent extension of existing postsynaptic spines during ProSAP1 or ProSAP2 overexpression is dependent on Abp1. In line with a role of Abp1 in transmitting signals from the PSD to Arp2/3 complex-mediated actin dynamics, our analyses show that ProSAP/Shank-mediated spine enlargements are not only dependent on Abp1 but also require a functional Arp2/3 complex. The fact that arresting the Arp2/3 complex in an inactive state by overexpression of the N-WASP C terminus and that knocking down either the Arp2/3 complex component Arp3 or the Abp1-binding Arp2/3 complex activator N-WASP disrupted ProSAP-induced head expansion strongly indicates that the Arp2/3 complex is an important effector for ProSAP-mediated morphology control in postsynaptic spines. Our study thus reveals that Abp1 with its dual role of interconnecting actin filaments and ProSAP/Shanks on one side and of mediating Arp2/3 complex-dependent actin dynamics on the other side is a crucial factor in the establishment of mature spines and the formation of synapses because it functionally coordinates both processes.

References

Boeckers TM (2006) The postsynaptic density. Cell Tissue Res 326:409–422.

Boeckers TM, Bockmann J, Kreutz MR, Gundelfinger ED (2002) ProSAP/Shank proteins—a family of higher order organizing molecules of the postsynaptic density with an emerging role in human neurological disease. J Neurochem 81:903–910.

Carlisle HJ, Kennedy MB (2005) Spine architecture and synaptic plasticity. Trends Neurosci 28:182–187.

Dillon C, Goda Y (2005) The actin cytoskeleton: integrating form and function at the synapse. Annu Rev Neurosci 28:25–55.

Du Y, Weed SA, Xiong WC, Marshall TD, Parsons JT (1998) Identification of a novel cortactin SH3 domain-binding protein and its localization to growth cones of cultured neurons. Mol Cell Biol 18:5838–5851.

Fenster SD, Kessels MM, Qualmann B, Wook JC, Nash J, Gundelfinger ED, Garner CC (2003) Interactions between piccolo and the actin/dynamin-binding protein Abp1 link vesicle endocytosis to presynaptic active zones. J Biol Chem 278:20266–20277.

Gundelfinger ED, Kessels MM, Qualmann B (2003) Temporal and spatial coordination of exocytosis and endocytosis. Nat Rev Mol Cell Biol 4:127–139.

Gundelfinger ED, Boeckers TM, Baron MK, Bowie JU (2006) A role for zinc in post-synaptic density asSAMbly and plasticity? Trends Biochem Sci 31:366–373.

Han J, Kori R, Shui JW, Chen YR, Yao Z, Tan TH (2003) The SH3 domain-containing adaptor HIP-55 mediates c-Jun N-terminal kinase activation in T cell receptor signaling. J Biol Chem 278:52195–52202.

Hering H, Sheng M (2001) Dendritic spines: structure, dynamics and regulation. Nat Rev Neurosci 2:880–888.

Hering H, Sheng M (2003) Activity-dependent redistribution and essential role of cortactin in dendritic spine morphogenesis. J Neurosci 23:11759–11769.

Kessels MM, Qualmann B (2002) Syndapins integrate N-WASP in receptor-mediated endocytosis. EMBO J 21:6083–6094.

Kessels MM, Qualmann B (2006) Syndapin oligomers interconnect the machineries for endocytic vesicle formation and actin polymerization. J Biol Chem 281:13285–13299.

Kessels MM, Engqvist-Goldstein AE, Drubin DG (2000) Association of mouse actin-binding protein 1 (mAbp1/SH3P7), an src kinase target, with dynamic regions of the cortical actin cytoskeleton in response to Rac1 activation. Mol Biol Cell 11:393–412.

Kessels MM, Engqvist-Goldstein AE, Drubin DG, Qualmann B (2001) Mammalian Abp1, a signal-responsive F-actin-binding protein, links the actin cytoskeleton to endocytosis via the GTPase dynamin. J Cell Biol 153:351–366.

Kreienkamp HJ (2002) Organisation of G-protein-coupled receptor signalling complexes by scaffolding proteins. Curr Opin Pharmacol 2:581–586.

Kuriu T, Inoue A, Bito H, Sobue K, Okabe S (2006) Differential control of postsynaptic density scaffolds via actin-dependent and -independent mechanisms. J Neurosci 26:7693–7706.

Larbolette O, Wollscheid B, Schweikert J, Nielsen PJ, Wienands J (1999) SH3P7 is a cytoskeleton adapter protein and is coupled to signal transduction from lymphocyte antigen receptors. Mol Cell Biol 19:1539–1546.

Le Bras S, Foucault I, Foussat A, Brignone C, Acuto O, Deckert M (2004) Recruitment of the actin-binding protein HIP-55 to the immunological synapse regulates T cell receptor signaling and endocytosis. J Biol Chem 279:15550–15560.

Matus A (2000) Actin-based plasticity in dendritic spines. Science 290:754–758.

Naisbitt S, Kim E, Tu JC, Xiao B, Sala C, Valtschanoff J, Weinberg RJ, Worley PF, Sheng M (1999) Shank, a novel family of postsynaptic density proteins that binds to the NMDA receptor/PSD-95/GKAP complex and cortactin. Neuron 23:569–582.

Okamoto K, Nagai T, Miyawaki A, Hayashi Y (2004) Rapid and persistent modulation of actin dynamics regulates postsynaptic reorganization underlying bidirectional plasticity. Nat Neurosci 7:1104–1112.

Pinyol R, Haeckel A, Ritter A, Qualmann B, Kessels MM (2007) Regulation of N-WASP and the Arp2/3 complex by Abp1 controls neuronal morphology. PLoS ONE 2:e400.

Qualmann B, Kelly RB (2000) Syndapin isoforms participate in receptor-mediated endocytosis and actin organization. J Cell Biol 148:1047–1062.

Qualmann B, Boeckers TM, Jeromin M, Gundelfinger ED, Kessels MM (2004) Linkage of the actin cytoskeleton to the postsynaptic density via direct interactions of Abp1 with the ProSAP/Shank family. J Neurosci 24:2481–2495.

Rostaing P, Real E, Siksou L, Lechaire JP, Boudier T, Boeckers TM, Gertler F, Gundelfinger ED, Triller A, Marty S (2006) Analysis of synaptic ultrastructure without fixative using high-pressure freezing and tomography. Eur J Neurosci 24:3463–3474.

Roussignol G, Ango F, Romorini S, Tu JC, Sala C, Worley PF Bockaert J, Fagni L (2005) Shank expression is sufficient to induce functional dendritic spine synapses in aspiny neurons. J Neurosci 25:3560–3570.

Sala C, Piëch V, Wilson NR, Passafaro M, Liu G, Sheng M (2001) Regulation of dendritic spine morphology and synaptic function by Shank and Homer. Neuron 31:115–130.

Schubert V, Da Silva JS, Dotti CG (2006) Localized recruitment and activation of RhoA underlies dendritic spine morphology in a glutamate receptor-dependent manner. J Cell Biol 172:453–467.

Sheng M, Kim E (2000) The Shank family of scaffold proteins. J Cell Sci 113:1851–1856.

Sheng M, Sala C (2001) PDZ domains and the organization of supramolecular complexes. Annu Rev Neurosci 24:1–29.

Strasser GA, Rahim NA, VanderWaal KE, Gertler FB, Lanier LM (2004) Arp2/3 is a negative regulator of growth cone translocation. Neuron 43:81–94.

Tada T, Sheng M (2006) Molecular mechanisms of dendritic spine morphogenesis. Curr Opin Neurobiol 16:95–101.

Yamabhai M, Kay BK (1997) Examining the specificity of Src homology 3 domain – ligand interactions with alkaline phosphatase fusion proteins. Anal Biochem 247:143–151.